Investigation of the Influence of Spacer Arm on the Structural Evolution of Affinity Ligands Supported on Agarose

Valentina Busini, Davide Moiani, Davide Moscatelli, Laura Zamolo, and Carlo Cavallotti*

Department di Chimica, Materiali e Ingegneria Chimica "G. Natta", Politecnico di Milano, Via Mancinelli 7−20131 Milano, Italy

Received: April 10, 2006; In Final Form: July 10, 2006

The influence of the spacer arm on the interaction between agarose and a supported ligand was investigated through molecular dynamics for a combination of several spacers. The spacers differ for degree of hydrophobicity, length, and chemical composition, which was varied through insertion of thio, ether, and CH_2 groups. Agarose was modeled through a modified Glycam force field, whose parameters were determined through ab initio calculations. The structural model of agarose used for the calculations was obtained through MD studies of the conformational evolution of several agarose single and double helixes. The simulations showed that a modification of the spacer properties could determine a change of the stable structure of the ligand with respect to the support. In particular, if the spacer is hydrophilic and rigid, the favored structure is with extended spacer and solvated ligand. Either increasing the spacer length, and thus its flexibility, or decreasing its solvation free energy, which corresponds to diminishing its affinity for water, rapidly leads to a conformational change in which the ligand adsorbs on agarose. Interestingly, we found that if the spacer is long and hydrophilic, a third metastable structure, in which the spacer is sandwiched between the ligand and agarose, is possible. Simulations of several ligands adsorbed on neighboring sites on agarose showed that if the support is not held fixed through restraints, the interaction force between vicinal ligands is sufficient to determine a major conformational change of the system.

1. Introduction

Affinity chromatography is an important separation process that has been amply exploited for the separation and concentration of the desired product from a complex mixture.[1] A chromatographic process is characterized by a mobile phase, a stationary phase, and a columnar geometry. Each of these parameters must be optimized to improve the performance of the separation process. For protein affinity separation, chromatographic media must have chemical and physical stability and an overall hydrophilic character and should not contain groups that bind proteins nonspecifically while still maintaining a reasonably high density of binding sites for spacers and ligands.[2,3] The stationary phase is usually composed of a substrate and a specific ligand covalently bonded to the support through a spacer arm to increase the capability of small ligands to reach difficult to access protein binding sites.[4]

Determining the optimal stationary phase for a given separation requires, in principle, experimentally evaluating each of the materials for the separation of interest. This is often done through a combinatorial approach by which different supports, spacers, and ligands are sequentially screened until an optimal conformation is found. A preferable alternative would be to develop a better understanding of the relationship between stationary-phase structural properties and performances, which might guide one toward a rational design of the affinity material. A first step in this direction has been the systematic investigation of the effect of the spacer arm length and composition on the binding and recovery of different enzymes and carbohydrates[3,5−8] in affinity chromatography separations. Some investigations have shown that a hydrophobic spacer can provide a site for nonspecific adsorption, which has generally been regarded as unwanted or deleterious in bioaffinity systems as the specificity of the affinity systems is reduced.[9] Attenuation of these unwanted hydrophobic interactions is typically achieved with shorter or more hydrophilic spacer arms. O'Carra[5] demonstrated that the presence of a hydrophobic spacer causes formation of nonspecific bonds of the substrate with several enzymes. This was shown when activating an agarose matrix (Sepharose 4B) with cyanogen bromide coupled with 1,3-diaminopropanol, and using an aminopropanol arm as spacer lengthened and functionalized with a variety of terminal groups. Chromatographic analyses were then performed using biospecific ligands and compared with results obtained with nonbiospecific ligands linked to the support via hydrocarbon spacer arms. It was found that the control gels could bond a wide range of enzymes, which indicated that the interactions were nonspecific. To validate this assumption a new generation of gels was prepared in which nonspecific ligands were bound to the surface via hydrophilic spacers, which resulted in a general loss of binding properties. This confirmed that in the previous experiments adsorption was determined by nonspecific interactions with the hydrophobic spacer. The same conclusions were drawn more recently by O'Flaherty et al.,[6] studying the mechanism of locking on to improve the selectivity of protein purification procedures based on immobilized cofactor derivatives. Despite the risk of loss of selectivity, a hydrophobic spacer has been used with success by several authors (Massoulié and Bon,[7] McCourt and Gustafson,[8] and Lowe[9]) to improve protein adsorption processes. The influence of the spacer arm on protein retention on a cation-exchange adsorbent has been recently investigated by De Phyllips et al., finding that a decrease of the spacer arm length

* To whom correspondence should be addressed. Phone: ++39-02-23993176. Fax: ++39-02-23993180. E-mail: carlo.cavallotti@polimi.it.

10.1021/jp0622278 CCC: $33.50
Published on Web 10/31/2006

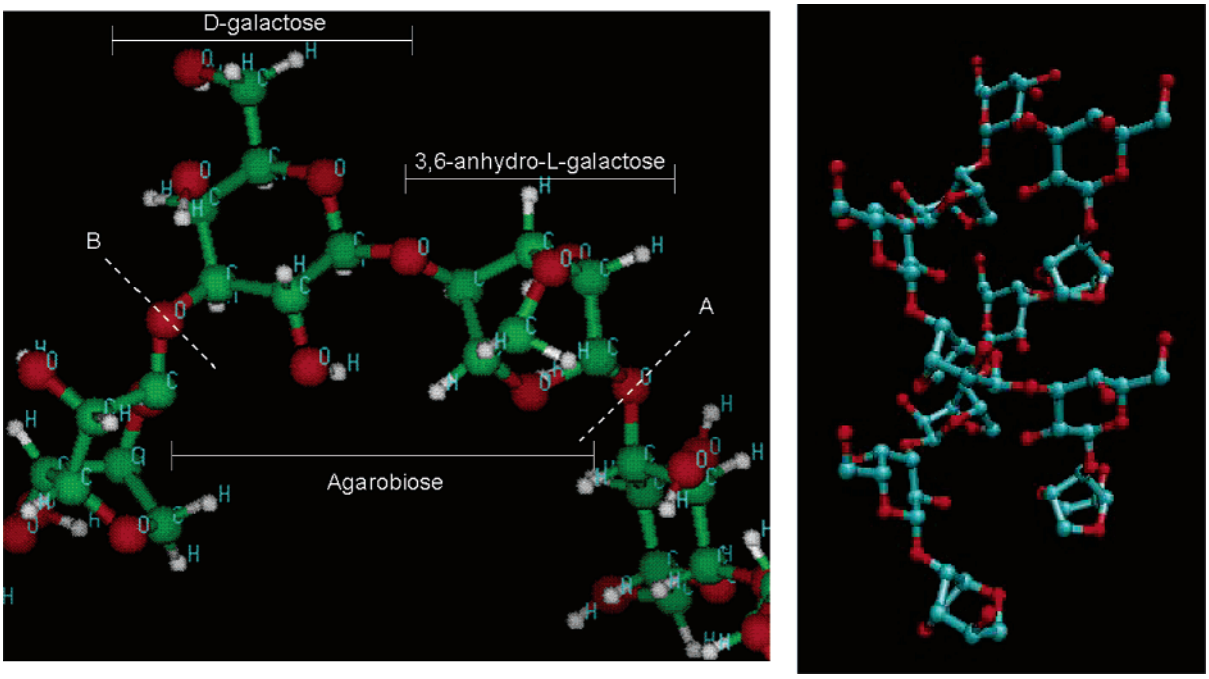

Figure 1. (a) Agarose unit and (b) double chain structure (1AGA from PDB). The 1,3−1,4 connectivity of the D-galactose and 3,6-anhydro-L-galactose units is explicitly evidenced.

can increase protein retention.[10] Similarly, Berna et al. found that a modification of the spacer chemical composition could determine the loss of adsorption capacity of cyanocarbon ligands known to selectively bind human serum proteins.[11]

Though experimental studies evidenced the influence of the spacer on the protein binding chemistry, it is difficult to determine the chemical physical origin of this effect. This is often the case for complex systems in which biomolecules interact with ligands bound to a solid support. Computational studies can help shed light on such systems as they allow identification and quantification of the nature of the intermolecular interaction of the supported molecules as well as determination of the minimum energy structure of the solid phase. An atomistic computational approach has, in fact, been recently used by Liapis and co-workers to investigate the structure and binding site availability of ion-exchange materials used for chromatography.[4,12]

In this framework, this work is focused on study of the conformational properties of the ligand−spacer−support system. The aim is to develop a computational framework that can be adopted to investigate how the chemical structure and length of the spacer used to connect the ligand to the support can influence its conformational evolution and study the interaction of affinity ligands with the support itself and among themselves.

First, a sufficiently general model of the support was chosen. The model must possess the general properties that characterize the materials usually adopted to support affinity ligands, such as availability of a reasonably high density of binding sites for spacers and ligands, chemical inertness with respect to proteins, and an overall hydrophilic character. Moreover, to be able to build a sufficiently reliable molecular model, its structure must be known or at least a sufficient amount of information about its morphology and three-dimensional conformation must be available. Given such requirements, the natural choice for the model support was agarose. Agarose is in fact widely used as substrate in protein purification for its particular properties, among which its particular gelling characteristics that allow agarose to form in aqueous environment gels that are more resistant than those generated by any other gel-forming agent

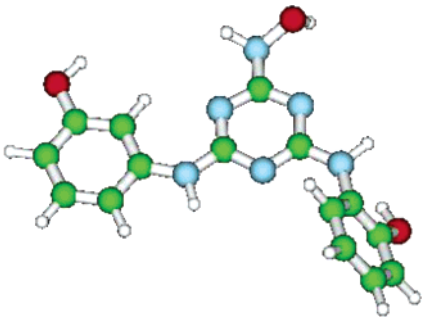

Figure 2. Structure of the A2P ligand considered in the simulations.

in equal concentrations. They are also very stable, preventing formation of undesired precipitates in the presence of reactive cations, can be used over a wide pH range (pH 3−13), and withstand thermal treatments very well, even above 100 °C, which allows good sterilization. In addition, agarose has several hydroxyl groups available for activation and derivatization, is hydrophilic, and generally does not interact with proteins. What is, however, most important from a molecular point of view is that much is known about agarose molecular structure, which is a fundamental requirement in order to build a reliable model of the support. Agarose molecular composition and structure are shown in Figure 1.

A further choice is that of the ligands that are to be investigated. We limited the field of investigation by studying in detail a known ligand that is of interest for affinity chromatography of monoclonal antibodies, specifically IgG. It is a disubstituted aminophenol derivative of trichlorotriazine whose structure is shown in Figure 2, which was discovered in ProMetic Life Science Inc. laboratories through screening of combinatorial libraries.[13] We will refer to this ligand in the following as A2P. The ligand is slightly hydrophobic and possesses hydroxyl groups that bind the protein. The experimental process that led to the development of A2P was aimed at developing a molecule that could still maintain the capability to bind the target protein while adsorbed on a support. The ligand is in fact known to be active when supported on agarose

or agarose-based gels, such as sepharose, which agrees with the support model chosen for the present investigation.

Several spacers of different composition and length were considered in the simulations. The spacers differ by the number of thio, ether, and CH_2 groups along the main chain, which are introduced with the intent of helping the ligand attain a solvated structure and increase its accessibility to proteins dissolved in solution. The spacer parameters were rationalized in terms of length and solvation free energy.

The paper is organized as follows. First, the computational approach used to investigate the interaction of the agarose substrate with ligands and spacers as well as details on the computational protocol we adopted are described in the Method and Theoretical Background section. Then the development of a model of the agarose structure to be used in the simulations is presented and discussed. Successively, we report the results of the studies on the influence of the spacer composition and length on the conformational evolution of the ligand−spacer−substrate system. The possibility that three ligands are adsorbed in neighboring positions on the same agarose chain is then investigated. All simulations were performed using A2P as the test molecule. In all the above simulations the rigidity of the agarose support was considered and its influence on obtaining a stable conformation was investigated, changing the number of agarose chains included in the support model and applying restraints on the agarose terminal groups. An energetic analysis was finally performed in order to identify the driving forces that determine the conformational evolution of the investigated systems.

The computational framework developed here and the simulations performed are to be considered as an intermediate step toward the final goal of simulating the supported ligand in the presence of the solvated protein. This has also dictated the choice of the force fields adopted for the simulations, Glycam[14] and Amber,[15] which were originally developed and optimized with the purpose of studying the protein dynamics.

2. Method and Theoretical Background

The nature of the interaction of affinity ligands and their spacers with the agarose support was investigated through molecular dynamic (MD) simulations. The force field adopted for the agarose support was Glycam 04,[14,16,17] developed to study the interaction of carbohydrates with proteins. Spacers and ligands were described using the Parm94 force field,[18] whose parameters (atom types) are consistent with those of Glycam. However, since the 3,6-anhydro-galactose unit is not defined in the standard Glycam force field, we modified it in order to include anhydro-galactose as a new unit. The minimal energy 3,6-anhydro-galactose structure was determined using density functional theory with correlation and exchange functional energy calculated using the B3LYP functionals and the 6-31g-(d,p) basis set. The optimized molecular conformation is shown in Figure 3.

The atomic types and intramolecular interaction parameters were defined from analogy with the original Glycam force field. Charges, atomic-type assignations, connectivities, and minimum energy bond distances and angles are summarized in Table 1, where they are reported following the same convention adopted in Glycam 04. In addition to the data of Table 1, atoms O5 C1 and O3 C6 were given the loop closure assignment.

The atomic partial charges reported in Table 1 were determined following the same approach adopted for the development of Glycam 04. Electrostatic potentials were calculated at the HF/6-31g(d) level, and charges were fit using the RESP formalism.[19] ESP values were determined on a grid of 1 point/Å^2 at 1.4, 1.6, 1.8, and 2.0 times the van der Waals radii and then fit through a two-step procedure to atomic charges, imposing a zero net charge on all aliphatic hydrogen atoms.

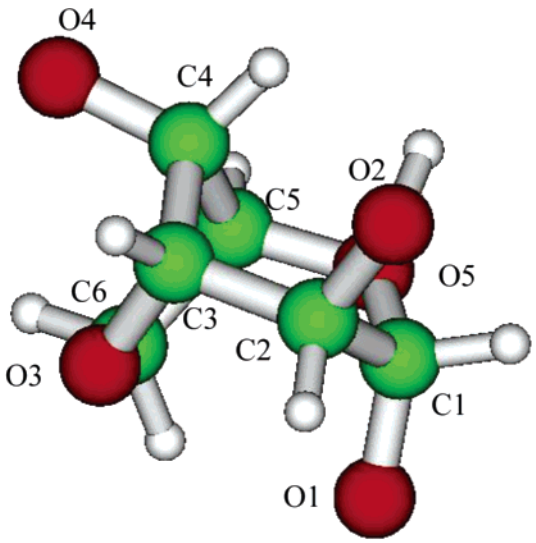

Figure 3. Structure of the 3,6-anhydro-galactose unit optimized at the B3LYP/6-31g(d,p) level. Atoms are numbered according to the conventional carbohydrate-numbering scheme.

TABLE 1: 3,6-Anhydro-galactose Molecular Parameters: Geometrical Parameters Calculated at the B3LYP/6-31g(d,p) Level, Atomic Charges As Described in the Text

atom no.	atom name	atom type	topol. type	connectivity and geometrical parameters						charge
1	DUMM	DU	M	0	−1	−2	0.000	0.0	0.0	0.0
2	DUMM	DU	M	1	0	−1	1.522	0.0	0.0	0.0
3	DUMM	DU	M	2	1	0	1.422	109.5	0.0	0.0
4	C1	CG	M	3	2	1	1.400	113.9	60.0	0.521
5	H1	H2	E	4	3	2	1.097	110.7	−56.2	0.0
6	C2	CG	M	4	3	2	1.549	107.4	−171.5	0.263
7	H2	H1	E	6	4	5	1.094	107.1	45.5	0.0
8	O2	OH	S	6	4	5	1.421	114.8	162.7	−0.738
9	H2O	HO	E	8	6	4	0.966	108.2	52.6	0.426
10	C3	CG	M	6	4	5	1.545	108.4	−73.0	0.370
11	H3	H1	E	10	6	4	1.093	110.9	172.1	0.0
12	O3	OS	E	10	6	4	1.448	110.8	52.1	−0.586
13	C4	CG	M	10	6	4	1.530	110.6	−61.0	0.115
14	H4	H1	E	13	10	6	1.092	114.8	−48.3	0.0
15	C5	CG	3	13	10	6	1.542	97.2	69.9	0.311
16	H5	H1	E	15	13	10	1.091	113.9	169.3	0.0
17	O5	OS	E	15	13	10	1.432	109.2	−71.3	−0.565
18	C6	CG	B	15	13	10	1.449	101.2	43.8	0.300
19	H61	H1	E	18	15	17	1.094	110.2	120.8	0.0
20	H62	H1	E	18	15	17	1.096	109.2	−120.2	0.0
21	O4	OS	M	13	10	6	1.415	112.7	−171.4	−0.417

Because of the rigidity of the anhydro-galactose unit and the presence of only one hydroxyl group, the large conformational search that was necessary for the development of the original Glycam force field could be limited in this case to study of the scan of the potential-energy surface corresponding to rotation of the hydroxyl group around the O−C bond. We found that rotational motion is almost unhindered and thus estimated the anhydro-galactose partial atomic charges averaging the RESP values they assume during H−O bond rotation over 12 different structures optimized at the HF/6-31g(d) level.

As specified in the Introduction, for the simulations we chose to use the agarose double helix as a model of the support material. In fact, its X-ray structure was determined by Arnott in 1974 and is reported in the Protein Data Bank as 1AGA.[20]

This structure proved to be stable in all molecular dynamics simulations we performed and thus was preferred to the bundle of single helixes that has been recently proposed as an alternative model.[21] We, in fact, tried to obtain a stable and ordered support model consisting of bundles of single helixes, but the results of all MD simulations led to formation of unaligned and disordered systems. In contrast, as will be discussed in the next section, simulations of bundles of two and three double helixes resulted in formation of stable and ordered systems, despite the relatively small time scale accessible for MD simulations of systems of this size (10−30 ns). Hydrogen atoms were added to the X-ray coordinates consistently with the chemical structure of the D-galactose or 3,6-anhydro-L-galactose, while the terminal residues were saturated with $O-CH_3$ groups.

The structure of the ligand considered in this study is shown in Figure 2. The ligand geometry was optimized before starting the MD simulations using density functional theory at the B3LYP/6-31g(d,p) level. Partial atomic charges were then determined using the RESP formalism on the electrostatic field computed through DFT. The general force field supplied in the amber suite was then used for the MD simulations using the electrostatic charges determined through quantum chemistry.[22]

Structures and atomic charges of spacers considered in the simulation were determined following the same procedure used for the ligands. Solvation free energies were determined on uncharged spacers using the IEFPCM implicit solvation model at the B3LYP/6-31g(d,p) level.

The complex agarose−spacer−ligand was solvated using explicit TIP3P water molecules adding a solvent shell of 12 Å.[23] This resulted in addition of about 5500 water molecules. A dielectric constant of 1 was used for all simulations, and the nonbonded cutoff was set to 10 Å. All simulations were performed using periodic boundary conditions, according to which the system is divided in unit cells of equal size. Long-range electrostatic interactions were evaluated using the particle mesh Ewald method, so that a particle within a unit cell interacts with all other particles in the same cell as well with all their periodic images in the other cells.[24] Advantages and disadvantages of Ewald boundary conditions have been recently discussed by Hunenberger and Cammon.[25] Of the several factors that were found to induce errors in the simulations, the only one that may be relevant to the present study is the fact that the solute size is not negligible with respect to that of the period cell, in particular for the agarose support model. The size of the periodic cell is in fact not sufficiently large to guarantee the absence of interactions between the head and tail of the agarose double chain. However, such interactions, rather then unrealistic, are indeed consistent with the fact that our agarose molecular model is a section of what is a much larger system. From this standpoint it is thus not correct to impose that the agarose ends are fully solvated since in the real system we intend to mimic they should be linked to a continuing agarose chain. The consistency of the simulations is further guaranteed by the fact that the part of the system under investigation is equally distant by both agarose ends and thus relatively insensitive to the limited size of the period cell along the agarose double helix axis direction.

The computational protocol adopted for the MD simulations is the following. First, a 2000-cycle minimization, in which the complex was restrained with a harmonic potential of the form $k(\Delta x)^2$, where Δx is the displacement and k the force constant, held fixed at 500 kcal/mol/Å^2 force, was performed to remove the initial unfavorable contacts made by the solvent. This was followed by a second 1500-cycle minimization without restraints. The temperature was then raised from 0 to 300 K by a simulated annealing of 20 ps at constant volume. To avoid wild fluctuations a weak restraint was imposed on the solute in this stage ($k = 10$ kcal/mol/Å^2). After heating the system, a 100-ps run was performed at constant pressure in order to permit the water density to relax. Finally, molecular dynamic simulations were performed for a standard period of 3 ns. The simulation time was significantly increased when the structural evolution of a bundle of two and three agarose chains was investigated. The SHAKE algorithm was used for all covalent bonds involving hydrogen, which allowed using a time step of 2.0 fs.[26] All simulations were performed at 300 K and constant atmospheric pressure.

Electrostatic and van der Waals solute−solvent interaction energies were calculated using the Anal program, of the Amber 8 computational suite, after reimaging to the original cell water molecules that diffused in periodic cells vicinal to that containing the agarose substrate and the adsorbed spacers and ligands. Medium energies were averaged on sets of 100 trajectories, corresponding to a time span of 100 ps.

Almost all simulations were performed using an agarose double helix composed of 108 residues as support model, whose length is about 15 nm. To evaluate how the double-helix mobility and flexibility can influence the conformational evolution of the system, MD simulations were first performed without restraints and then applying a restraining force constant of 10 kcal/mol/Å^2 on the terminal residues of the agarose chain. The magnitude of the restraining force was chosen so that the terminal groups of agarose were immobilized in space. A molecular model with limited flexibility is in fact expected to describe better a highly cross-linked agarose gel, which is that most often used in affinity chromatography.

All molecular dynamics simulations were done using the Amber 8 computational suite,[15] while the ab initio simulations were performed with Gaussian 03.[27] Structures reported in this paper were produced using Molden 4.4[28] and VMD 1.8.2.[29]

3. Results and Discussion

The computational results are presented in four different sections, which correspond to the building blocks of this work. First, the agarose support structural model is developed and discussed. Then it is applied to simulate the conformational evolution of A2P bound through different spacers to a D-galactose agarose unit. Simulations were performed with and without imposing restraints on the terminal agarose units, though only the results of the restrained simulations are presented as they are expected to better describe the rigidity of the support material. Only in some significant cases are the results of simulations with unrestrained agarose reported. Finally, an energetic analysis is performed to identify the driving forces that determine the system conformational evolution.

3.1. Development of the Agarose Structural Model. Agarose gels are among the most used support materials for protein affinity chromatography. Agarose is a neutral, long-chain polymer formed by β-D-galactopyranose residues 1,3-linked with 3,6-anhydro-L-galactose residues 1,4-linked. Both residues are repeated alternatively. The molecular weight assigned to non-degraded agarose is approximately 120 000. While the structure of agarose gels is still disputed, much more is known about that of the chemically similar carrageenan, which has been investigated experimentally and theoretically.[30] X-ray diffraction data have shown unambiguously that the predominant structural features in carrageenan gels are right-handed double helixes, while computational and NMR investigations seem to indicate

that conformational angles of statistically disordered chains deviate only slightly from that of ordered helix structures.[30,31] However, agar differs from kappa and iota carrageenan as the 3,6-anhydro-D-galactose residue is substituted by 3,6-anhydro-L-galactose. X-ray diffraction patterns of agarose were interpreted, in analogy with carrageenan gels, in terms of aggregates of double helixes,[20] left-handed, with a helix pitch of 26 Å. This is shorter than that of carrageenan, which was attributed to the lower content of sulfate groups that possibly cause a tighter and more compact conformation. The agarose chain structure is reported in Figure 1b, while the agarobiose disaccharide structural unit and its 1,3−1,4 connectivity have been evidenced in Figure 1a.

The gelation model currently accepted in the literature suggests that during the gelation of agarose left-handed double helixes are formed and then aggregate in bundles held together in a relatively ordered structure by hydrogen bonds.[32] Recently the structure model proposed by Arnott has been questioned on the basis of polarimetry and neutron scattering small-angle measurements performed during the thermoreversible gelation of agarose.[33] The collected data seem to indicate that the X-ray diffraction patterns of Arnott can be explained also in terms of a network of spatially ordered single-helix structures. However, these data have been measured in the agarose sol state and do not exclude the possibility that the double-helix structure, on the basis of which agarose gel properties are usually described, is formed during gelation. Computational investigation has, in fact, confirmed that the left-handed, double-helical structure is the most energetically stable one.[34] Interestingly, it has also been proposed recently that a better explanation of experimental data is obtained if it is assumed that a certain amount of loose single or double helixes is present in the gel.[35] These structures would be characterized by high mobility, and it is reasonable to assume that the ligands they support might behave differently than those linked to the cross-linked agarose units.

To develop the agarose structural model to use in the successive simulations we adopted the following approach. First, we simulated through MD the structural evolution of two parallel single helixes to investigate whether they might form an aligned ordered linear structure. The single-helix starting geometry was obtained using as input the 1AGA pdb double-helix structure, canceling one of the two helixes, and saturating the final residues with oxymethyl group. Successively the two double helixes were put in parallel positions. Though a relatively large time span of 20 ns was investigated, we did not obtain the expected result. The structure produced by the simulations was in fact only partially aligned, with the remaining portions of the two double helixes coiled around the inner core. It must, however, be pointed out that the results of these simulations were probably vitiated by the relative too small dimension of the adopted solvation box. In fact, especially in the initial steps of the simulations, the single helixes had a high mobility, which corresponds to a correlation length probably larger than the dimensions of the system we could consider because of computational limitations.

Successively we considered the left-handed double helix structure proposed by Arnott as the agarose model, for which the X-ray 1AGA structure is available in the PDB. Simulations revealed, not surprisingly, that the system is stable and rigid in the time frame considered for the simulation (3 ns), though some instability toward formation of large coils could be observed for longer simulations. Deformation of the helix could however be prevented by applying restraints on the four terminal units. The restrained system, constituted of 108 galactose units and about 15 nm long, was adopted in most of the simulations described in the next section. The size of the unit cell for a typical simulation is about $45 \times 40 \times 125$ Å^3.

Finally, we investigated whether we could produce a molecular model that might better describe the large bundles of helixes that are supposed to be the basic structure of the agarose gel. For this purpose we performed long (30 ns) simulations of two and three double helixes starting from parallel positions. Snapshots of the intermediate structures are reported in Figures 4 and 5. As can be observed, the first of the two simulations was started with the two helixes put in parallel positions and resulted in the ordered structure shown in Figure 4. This structure has the characteristics of stability, macroscopic order, and high surface area that are known to belong to agarose. In fact, only the first 15 ns of the simulation are shown in Figure 4, as for the successive 15 ns the structure remained practically unchanged. The two double-helix bundle structure generated by the 15-ns MD run was used in some of the successive simulations to investigate the effect of the size of the support model. The MD simulation (Figure 5) of three double helixes, starting from an aligned and parallel conformation, led to formation of a macroscopic system in which the agarose double helixes are strongly interacting. However, the ordered domains are characterized by the alignment of not more than two double helixes at the same time. This might be due to the insufficient simulation time, which, though large for a MD simulation (30 ns), is still small with respect to the typical folding time of molecules (microseconds). A more interesting hypothesis is that the agarose double helixes interact more easily in couples than in triples and that formation of large bundles is preceded by an initial formation of couples, which then aggregate.

Several simulations were performed with ligands adsorbed on agarose molecular models containing one and two double helixes. Similar results were obtained when we adopted the agarose model consisting of one double helix if its mobility was limited through application of restrains. This structural model, because of its smaller size, was thus adopted in most of the simulations reported in the next section.

3.2. Simulation of A2P Linked to Agarose through Different Spacers. The conformational evolution of A2P supported on agarose through spacers of different length and chemical composition was investigated through 3-ns MD simulations. Unless explicitly mentioned, the agarose structural model adopted in all simulations is the 108-residue double-helix structure that was described in detail in the previous section. The chain-end mobility was restrained through application of restraints, as previously specified. Simulations were started with the ligand fully solvated and the spacer extended with its axe normal to that of the support. Three different families of spacers, which differ by the number of CH_2, amine, and thiol group and their succession along the spacer chain, were considered. The investigated structures are summarized in Table 2. Spacers are covalently bonded to the epoxy-activated lateral CH_2OH groups of the D-galactose units of agarose through an $AgaCH_2O-CH_2-CHOH$ bond. The A2P ligand is also covalently bonded to the spacer through a NH or S bond to the free carbon atom of the triazinic ring.

An important parameter to discriminate the properties of the different spacers is hydrophobicity. As it is difficult to define an absolute hydrophobicity scale, we prefer to classify the different spacers in terms of their solvation free energy, which we calculated through quantum chemistry at the B3LYP/6-31g-(d,p) level using the implicit IEFPCM solvation model.[36] The computed data are collected in Table 2.

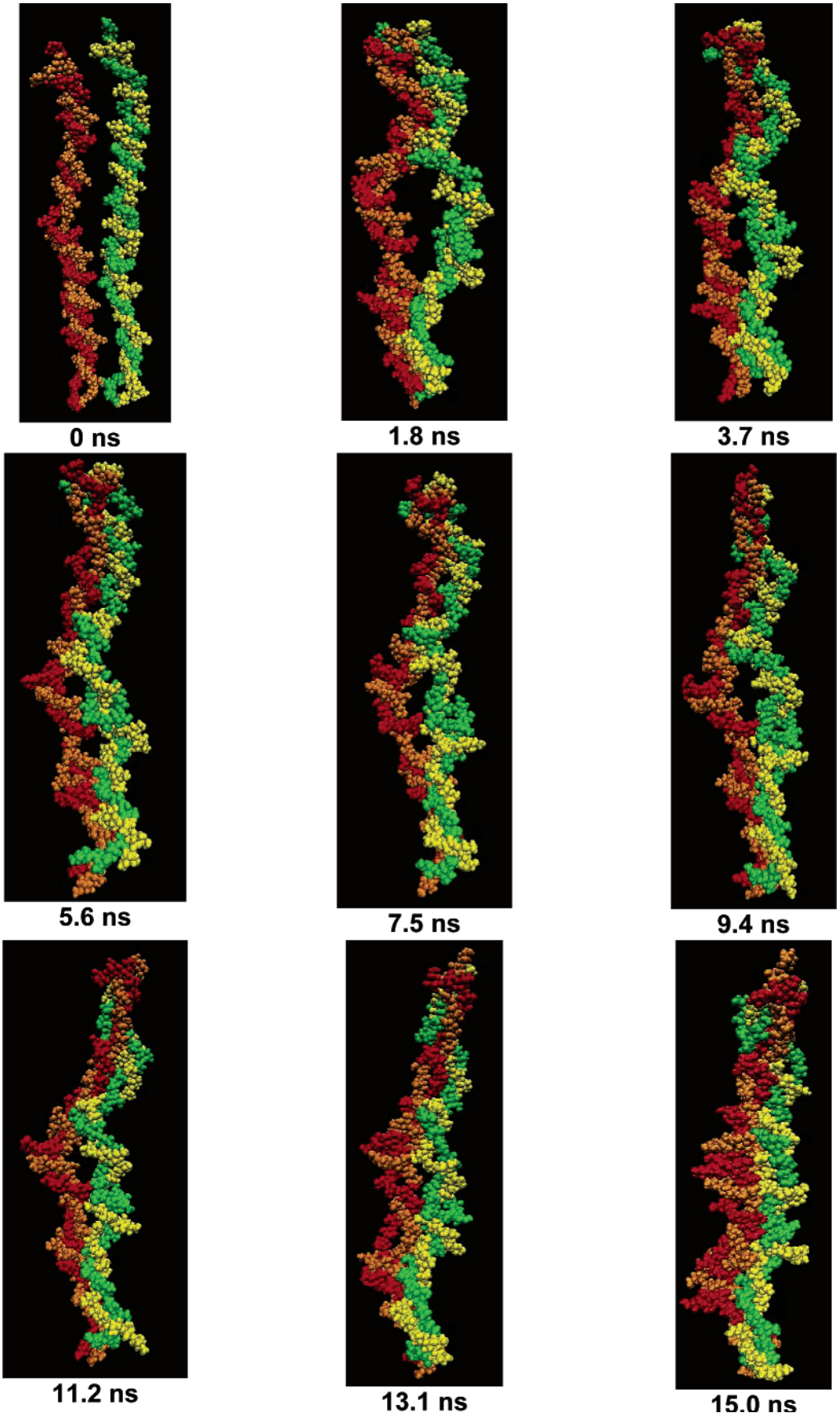

Figure 4. Snapshots of the first 15 ns simulation performed of two 108-unit agarose double helixes.

The first simulations we performed concerned the standard ligand−spacer−substrate conformation used by ProMetics, in which A2P is bound to the support by means of a CH_2−CHOH−CH_2−NH_2−$(CH_2)_2$−NH spacer. This spacer is characterized by a hydrophobic part, constituted by the three CH_2 groups, and a hydrophilic portion, mainly located in proximity

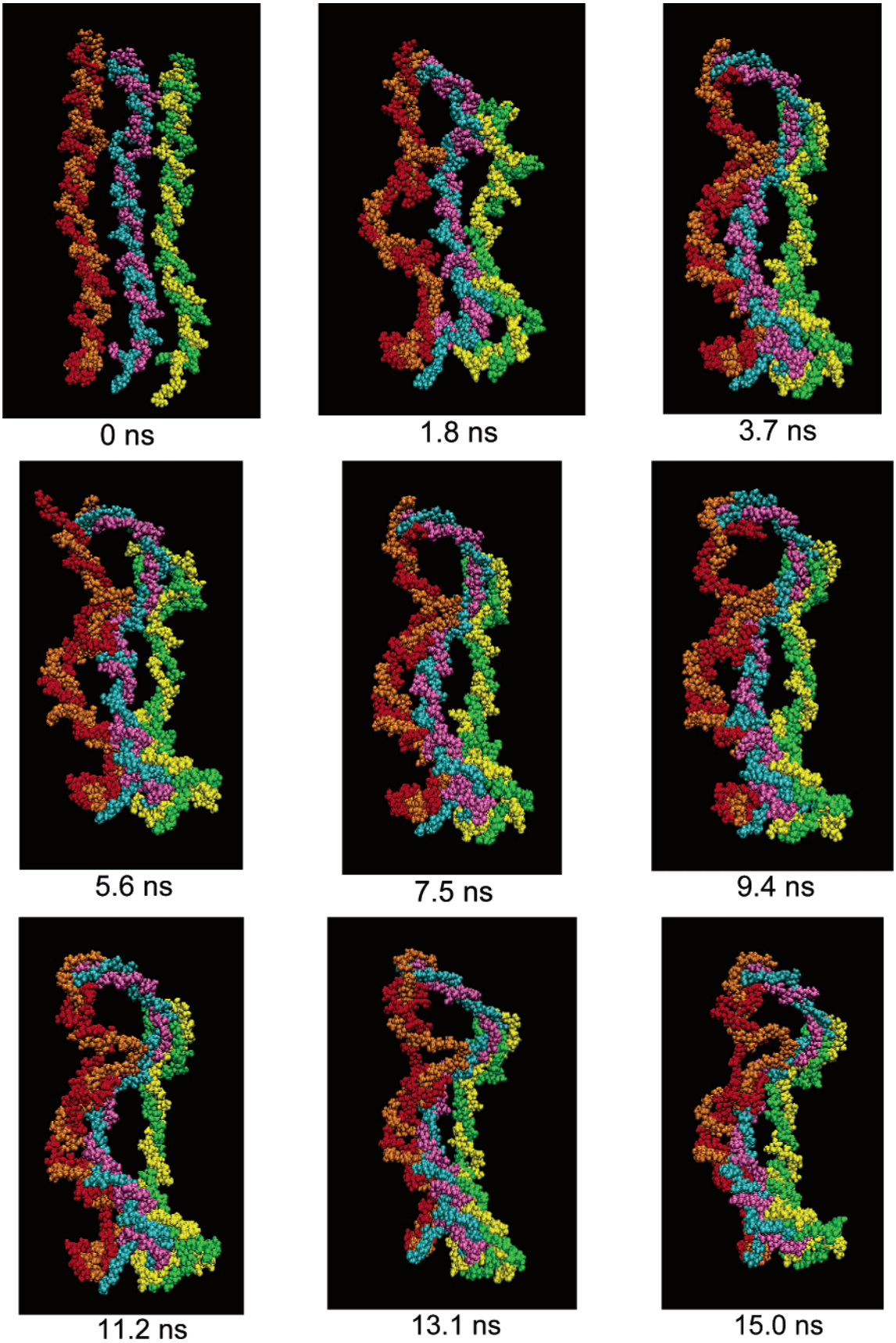

Figure 5. Snapshots of the first 15 ns simulation performed of three 108-unit agarose double helixes.

of the support and constituted essentially by the positively charged NH_2 group. The simulations were run for 3 ns and clearly showed that, already after the first nanosecond, the A2P ligand abandons the initial conformation and bends toward the substrate to form a rather stable complex with agarose. The time evolution of the minimum distance of the N atom of the triazine ring opposite the spacer and the agarose substrate is shown in Figure 6. The minimum distance parameter is defined as the

TABLE 2: Summary of Examined Conformations and Computed Spacers Free Solvation Energies. $CH_2-CHOH-CH_2-NH-(CH_2)_x-NH$ Free Solvation Energies Determined for Unprotonated and Uncharged Molecule

ligand		spacer	solvation free energy (kcal/mol)	length (Å)
2LP	A2P	$CH_2-CHOH-CH_2-NH-(CH_2)_2-NH$	2.59	6.6
6LP		$CH_2-CHOH-CH_2-NH-(CH_2)_6-NH$	3.13	11.4
8LP		$CH_2-CHOH-CH_2-NH-(CH_2)_8-NH$	4.42	13.9
SS3	A2P	$CH_2-CHOH-CH_2-S-(CH_2)_3-S$	−4.00	9.5
SS5		$CH_2-CHOH-CH_2-S-(CH_2)_5-S$	−2.72	12.0
DES	A2P	$CH_2-CHOH-CH_2-S-(CH_2)_2-O-(CH_2)_2-O-(CH_2)_2-S$	−4.25	15.1

distance between the mentioned N atom and the nearest atom of the agarose support. Simulations performed without applying restraints on the agarose chain ends evidenced a significant mobility of the double chain, which however did not lead to a major conformational change of its structure in the investigated time span. This high mobility is known to be a characteristic of agarose, as testified by experimental evidence that suggests the existence of a certain amount of highly mobile loose chains in the agarose gel.[35]

As we did not observe formation of any specific stable hydrogen bond between ligand and support, the nature of the interaction between agarose, the spacer, and A2P can be considered to be mainly hydrophobic. It is also important to observe that the hydrophilic NH_2 group is located in proximity of the surface, and its interaction with water is likely to be unaffected by the orientation of the relatively far A2P ligand. We verified that the influence of the NH_2 group of the spacer on the overall complex conformation is of secondary importance by performing MD simulations in which NH_2 was replaced with the much less hydrophilic uncharged NH group. The results were substantially unaffected by this substitution.

To study the influence of the spacer length on the A2P conformation, simulations were performed increasing the total number of CH_2 groups in the spacer from 2 to 6. The results of the simulations are shown in Figure 7.

The overall geometrical complex evolution is similar to that observed for the smaller ligand. A stable conformation in which A2P is adsorbed over agarose is reached in less than 1 ns and maintained throughout the successive 2 ns of simulation. A similar result is also obtained when two more CH_2 units increase the spacer length. These results, shown in Figure 8, seem to indicate that if a hydrophobic ligand, such as A2P, is bound to an agarose support through a hydrophobic spacer, it will reach in a brief period a stable conformation in which it is adsorbed on the surface. This indicates that for this ligand−spacer−substrate conformation the system must be considered as a whole in order to correctly describe its interaction with proteins and, in particular, large molecules such as monoclonal antibodies. It appears, in fact, reasonable that upon formation of the bond between the affinity material and the MAB, this large protein will interact contemporarily with the ligand and the support.

From this point of view the influence of the spacer should be regarded from a different standpoint. It is, in fact, evident from the analysis of Figures 6−8 that the spacer does not function to disperse the ligand in solution but is adsorbed almost entirely on the support and directly faces the liquid phase. It is thus accessible to the dissolved proteins and can contribute directly to the protein binding process. This is particularly relevant for the positive NH_2 group located at the base of the spacer. In fact, in the stable conformation predicted by the MD simulations, its possible interaction with the protein is not sterically hindered.

The second family of spacers investigated is constituted by the two thiophilic $CH_2-CHOH-CH_2-S-(CH_2)_x-S$ spacers. These spacers are more hydrophilic than those previously examined, as shown by the solvation free energies reported in Table 2, which are negative and increase with the number of CH_2 groups from −4.0 to −2.7 kcal/mol. The results of the MD simulations, shown in Figures 9 and 10, indicate that the stable structure of the A2P−spacer system with respect to the agarose support is sensitive to the length of the spacer. In particular, we chose to report in Figure 9 the results of the simulations in which the agarose motion has not been limited by restraints. The main difference between restrained and unrestrained simulations is the much higher mobility of the system. While restrained simulations probably better reproduce the rigidity of a cross-linked support material, unrestrained simulations allow one to more efficiently sample the confor-

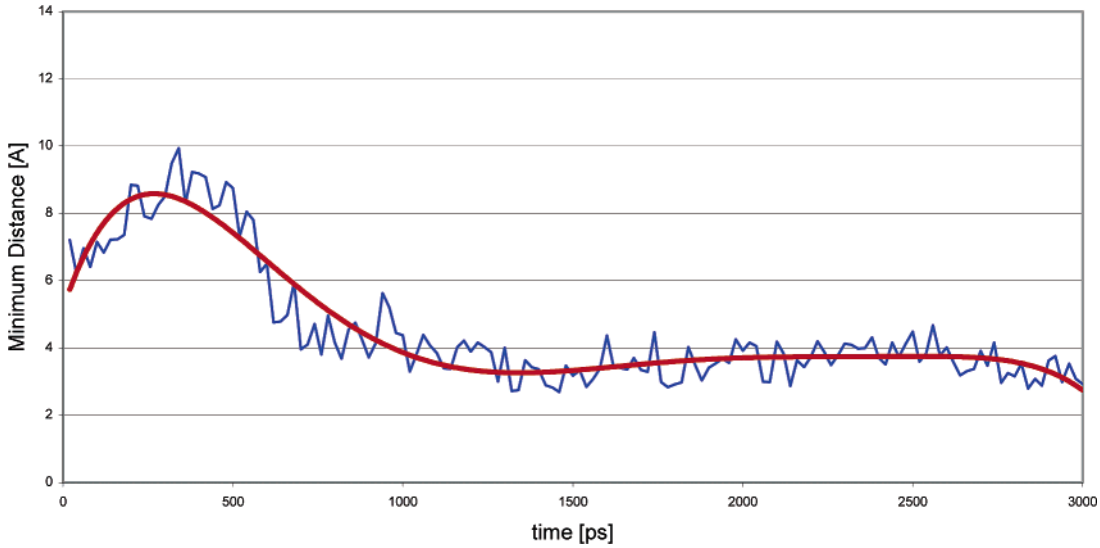

Figure 6. Temporal profile of the minimum distance between a target atom (N of the triazine ring para with respect to the spacer) of A2P and the agarose support to which it was connected through the $CH_2-CHOH-CH_2-NH_2-(CH_2)_2-NH$ spacer.

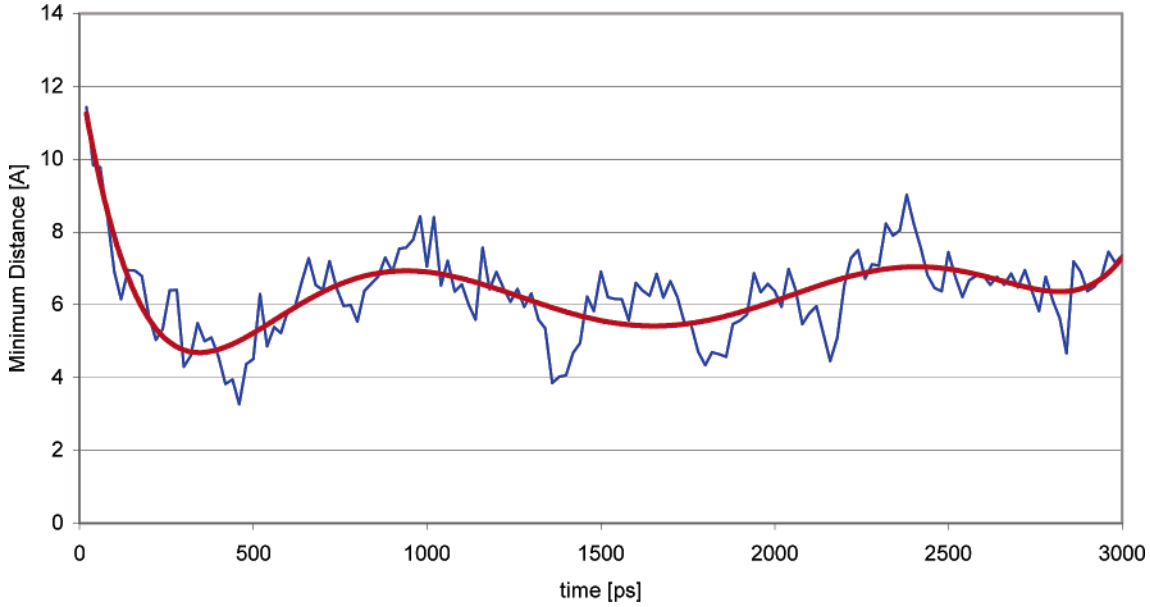

Figure 7. Temporal profile of the minimum distance between a target atom (N of the triazine ring para with respect to the spacer) of A2P and the agarose support to which it was connected through the $CH_2-CHOH-CH_2-NH_2-(CH_2)_6-NH$ spacer.

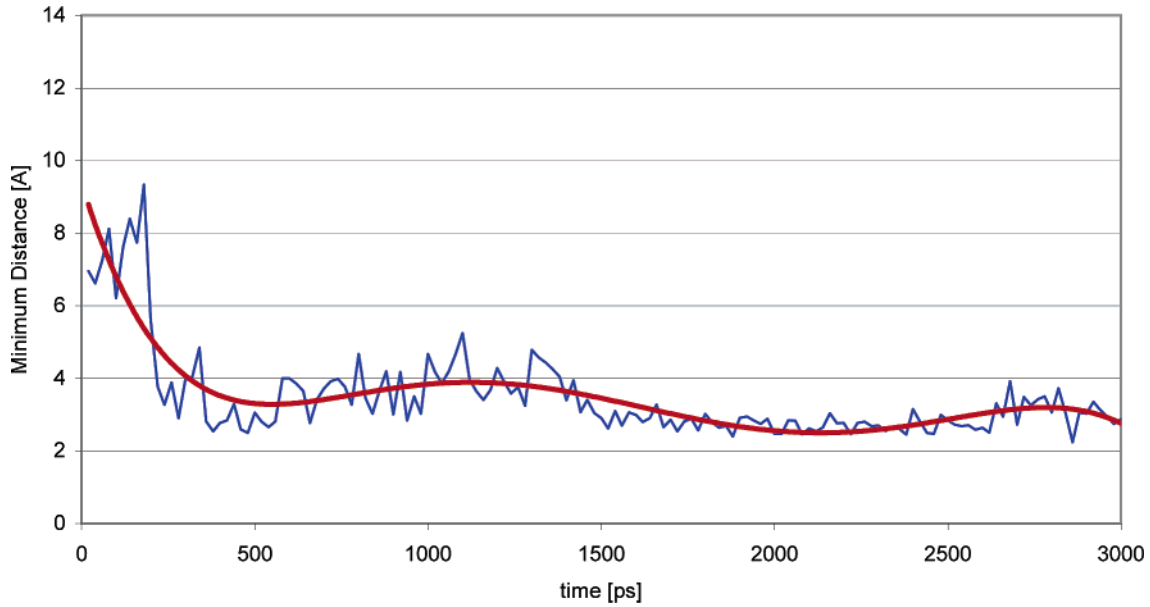

Figure 8. Temporal profile of the minimum distance between a target atom (N of the triazine ring para with respect to the spacer) of A2P and the agarose support to which it was connected through the $CH_2-CHOH-CH_2-NH_2-(CH_2)_8-NH$ spacer.

mational space. It is interesting to observe that the A2P−agarose distance has two minimum values in which A2P is at about 6 and 4 Å from agarose. In spite of this, it moves back to the liquid phase in both cases. This seems to indicate that the most stable conformation of the system is with the stretched spacer and A2P distanced from the support. This was the conformation maintained by A2P throughout the 3 ns in the simulations performed with the restrained system, whose time−distance graphic would thus appear as a straight line centered at about 10 Å. It is also interesting to relate the agarose−ligand distance fluctuations to the change of the internal energy of the spacer. For this purpose the sum of bond, angle, and dihedral energies of the spacer are reported in Figure 9b. It can be observed that a decrease of the A2P−agarose distance corresponds to a slight increase of the spacer energy, which suggests that the driving force that brings the ligand back in solution might be the internal strain of the spacer with respect to the most relaxed positions, in which it is completely extended. An alternative explanation is that thermal effects determine the ligand fluctuations. However, we observed that thermal fluctuations of the extent reported in Figure 9 usually led, for the other spacers investigated, to adsorption of A2P on agarose, which was not the case for the SS3 spacer and thus suggests that a different mechanism is active.

Given these observations it was very interesting to obtain a very different result when studying the similar $CH_2-CHOH-CH_2-S-(CH_2)_5-S$ spacer. In this case, in fact, both restrained and unrestrained simulations predicted that the most stable conformation is that with A2P positioned in proximity of the surface. This different behavior is probably the result of not only the different degree of hydrophilicity of the spacer arm, but also the higher mobility and flexibility of a longer spacer. It is, in fact, not surprising that a system with a high number of rotational degrees of freedom, such as that represented by the spacer considered here, will try to reach a minimum energy conformation in which the spacer arm is solvated and the ligand

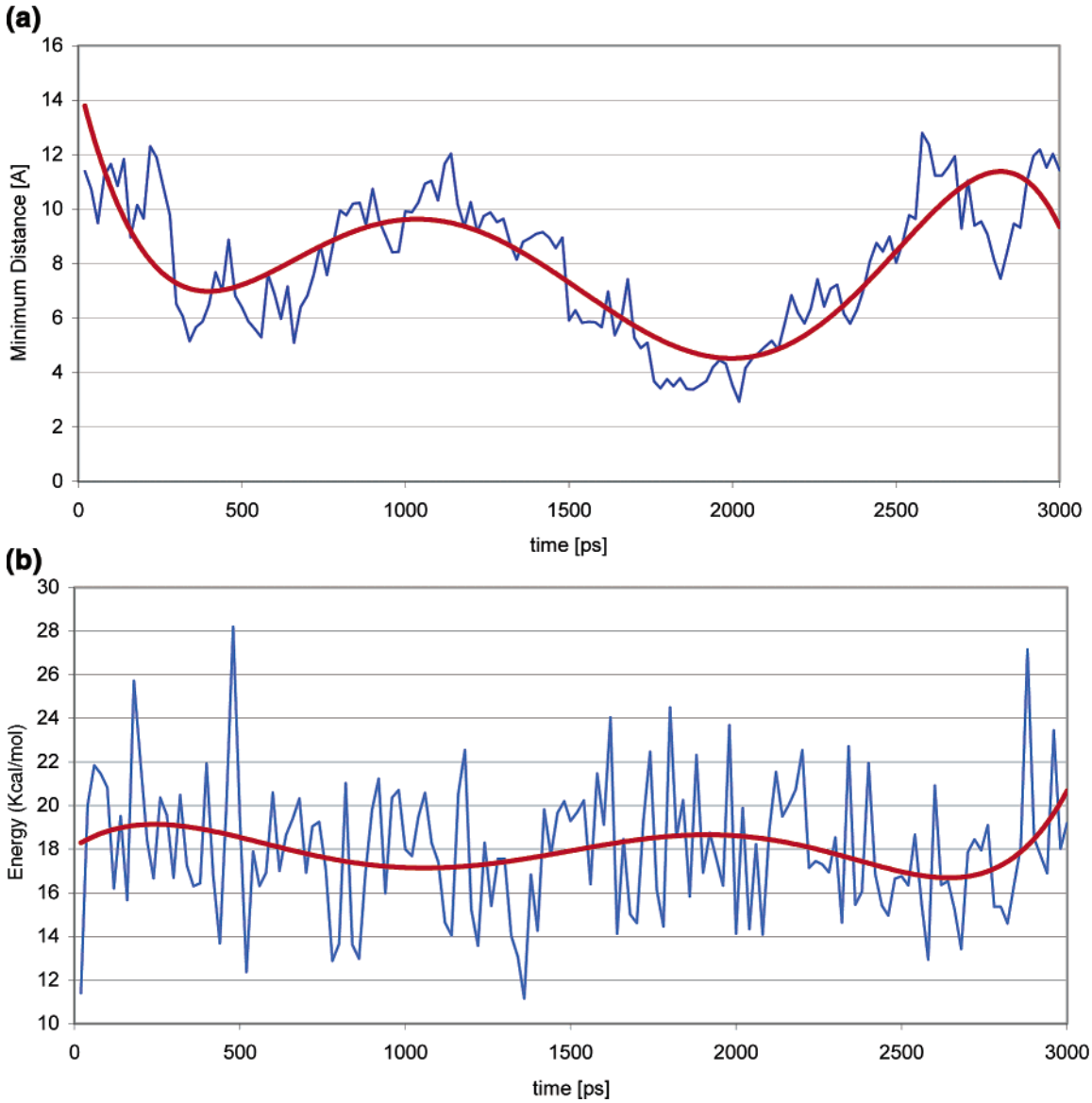

Figure 9. (a) Temporal evolution of the minimum distance between a target atom (N of the triazine ring para with respect to the spacer) of A2P and the agarose support to which it was connected through the $CH_2-CHOH-CH_2-S-(CH_2)_3-S$ spacer. The agarose surface model is not held fixed by restraints. (b) Time evolution of the spacer energy (bond + angle + dihedral).

interacts with the surface. From a more general point of view, it is interesting to comment on how a system whose stable conformation is that with the ligand partially adsorbed on the support material might bind a dissolved protein. The binding process can be judged from two standpoints: kinetic and thermodynamic. From a kinetic point of view, formation of a bond between protein and ligand requires that the ligand desorbs from the surface and moves toward the protein binding site. Though this might complicate the bond-formation process, it must however be pointed out that the time scale for the desorption of the ligand, which would probably be triggered by the approach of a protein to the support, is probably small if compared to that usually required for formation of intermolecular bonds. The thermodynamic effect might be, on the other hand, more important. In fact, attainment of a stable conformation in which the ligand is interacting with the support corresponds to an overall decrease of the free energy of the system, which should be overcome in order to let the ligand interact with a protein binding site.

The third system considered was A2P bound to the long and hydrophilic $CH_2-CHOH-CH_2-S-(CH_2)_2-O-(CH_2)_2-O-(CH_2)_2-S$ spacer. The results of the simulations are shown in Figure 11. This system has been the most investigated one in this study, essentially because of the scattering of the results. This ample conformational search showed that three different conformations are possible: A2P adsorbed on the surface with solvated spacer, A2P fully solvated with stretched spacer, and A2P aligned parallel to the support with the spacer positioned between the two structures. The last structure corresponds to the diagram reported in Figure 11, while the three different stable structures for this system are represented in Figure 12. Two of the three molecular representations shown in Figure 12 were obtained through MD simulations performed with the support model made of two double helixes obtained through the 30-ns run described in the previous section. The larger model of the support was in fact used in this case to investigate the sensibility of the investigated structural model to the size of the support model used in the simulation. The results were essentially similar to those obtained with the standard support model. The conformational evolution of this system can be interpreted as intermediate between that found with the $CH_2-CHOH-CH_2-S-(CH_2)_3-S$ and $CH_2-CHOH-CH_2-S-(CH_2)_5-S$ spacers.

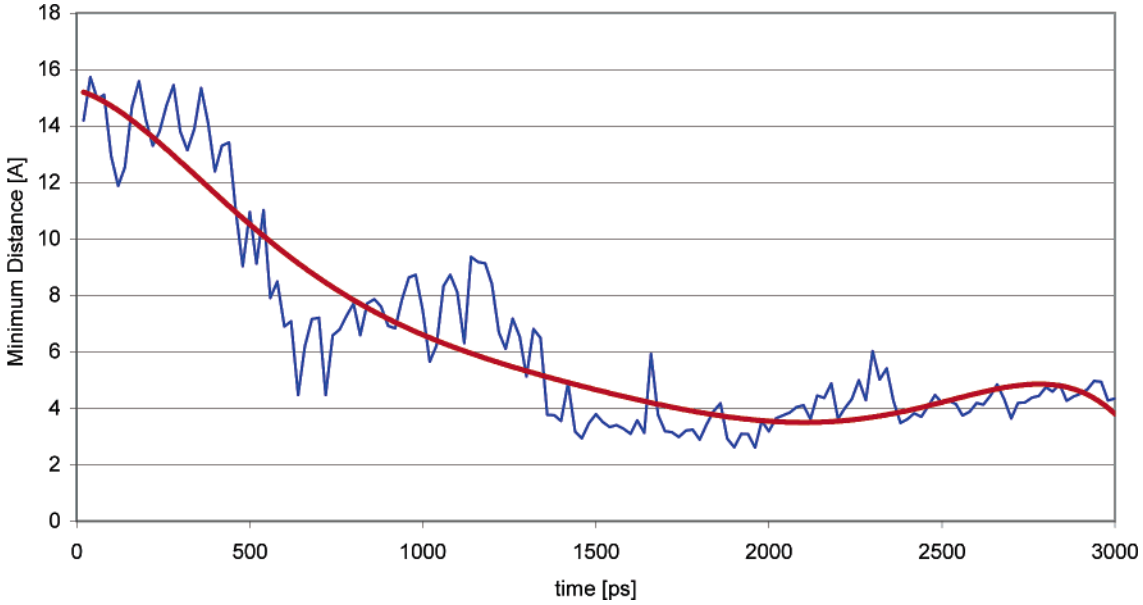

Figure 10. Temporal evolution of the minimum distance between a target atom (N of the triazine ring para with respect to the spacer) of A2P and the agarose support to which it was connected through the $CH_2-CHOH-CH_2-S-(CH_2)_5-S$ spacer.

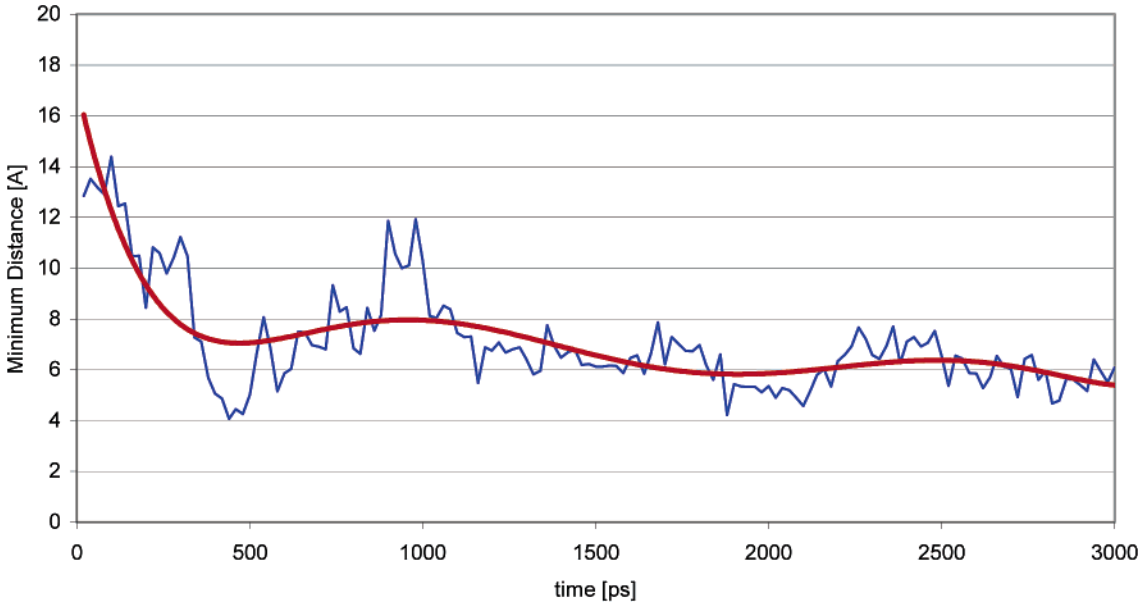

Figure 11. Temporal profile of the minimum distance between a target atom (N of the triazine ring para with respect to the spacer) of A2P and the agarose support to which it was connected through the $CH_2-CHOH-CH_2-S-(CH_2)_2-O-(CH_2)_2-O-(CH_2)_2-S$ spacer.

On one side the spacer arm would prefer, from an energetic and entropic point of view, to assume an elongated and solvated conformation. On the other, the spacer is sufficiently long so that several conformations are possible in which it is relatively unstrained and water coordinated even when the ligand is interacting with the support. However, given the high mobility of this system, it is likely that in the presence of a protein the ligand would easily leave the agarose surface and move toward the more hydrophobic surface offered by the protein.

In Figure 13 we summarize the results of the simulations described in this paragraph. In particular, we differentiated spacer effects in terms of flexibility and hydrophobicity, which, due to the difficulties in quantifying these variables, are simply represented in terms low (+), average (++), and high (+++) values. Hydrophobicity was considered low, average, and high if the relative solvation free energy found was less than −2 kcal/mol, between −2 and 2 kcal/mol, or higher than 2 kcal/mol, respectively. In the same way flexibility was defined as low when the spacer length was less than 10 Å, average when between 10 and 12 Å, and high when longer than 12 Å. The results are rationalized in terms of four different zones.

3.3. Investigation of the Interaction between Neighboring Supported Ligands. To investigate the possibility that ligands bound on neighboring sites might interact between themselves, we performed a simulation in which we attached three A2P ligands to the 108-residue agarose double helix, which corresponds roughly to 1 ligand for every 15 sites available for ligand binding. The spacer adopted to connect A2P to agarose was $CH_2-CHOH-CH_2-NH_2-(CH_2)_8-NH$. Simulations were performed with both restrained and unrestrained agarose. The final snapshot of the unrestrained MD simulations, which were run for 5 ns in order to allow the system the time to evolve to a stable conformation, is reported in Figure 14. As observed, these simulations clearly show that in such conditions formation of a strong interaction between two neighboring A2P ligands is possible, though it involves rearrangement of the agarose chain.

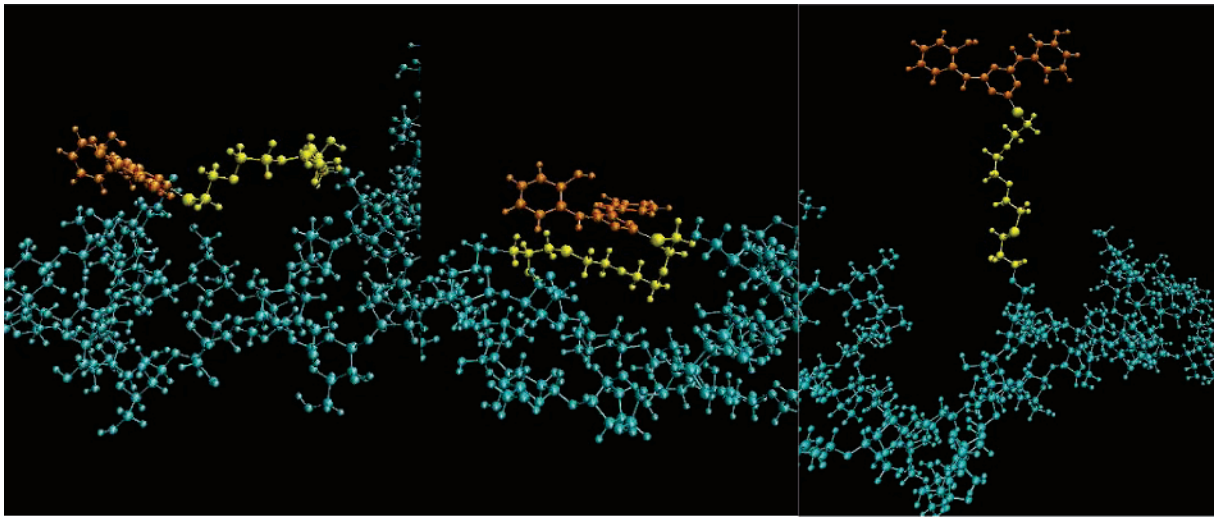

Figure 12. Structures of three stable conformations of A2P linked to agarose through the $CH_2-CHOH-CH_2-S-(CH_2)_2-O-(CH_2)_2-O-(CH_2)_2-S$ spacer: adsorbed with solvated spacer, spacer included between ligand and support, and solvated system.

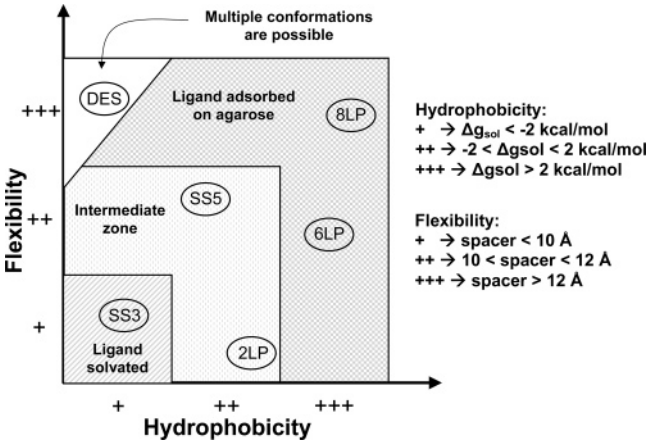

Figure 13. Schematic rationalization of the results of the simulations.

This result suggests that formation of intermolecular interactions between ligands adsorbed in proximity might be a driving force for a conformational change, provided that the agarose support has sufficient mobility. This is usually not the case for most of the agarose gel, as it is known, as discussed in the Introduction, that it is prevalently organized in bundles of double (or single) helixes, which probably have limited mobility. However, it has been shown experimentally[35] that agarose gels can contain several chains that are loose and thus free to move. Such chains would have a mobility very similar to that of the unrestrained double helixes considered in this study and might thus form structures comparable to those shown in Figure 14. Simulations performed with restrained agarose did not show, as expected, any interaction between the ligands.

3.4. Energetic Analysis. Interaction of the supported ligands and spacers with agarose and the encapsulating water environment was quantitatively investigated determining electrostatic and van der Waals interaction energies. The considered conformations are those described in the previous paragraphs. The aim of this energetic analysis is to try to quantitatively identify the driving force that determines the transition from a fully solvated structure of the supported ligand, which for A2P was obtained only using the SS3 spacer, and the conformation in which the ligand is adsorbed on agarose or interacting with the spacer itself. An important indication in this direction can be obtained comparing the electrostatic and van der Waals energies of interaction of bound A2P and of the different spacers considered in this study with those of the same ligands and spacers solvated with water. To avoid fictitious interactions between ligands and spacers, different MD simulations were performed for each ligand and spacer, immersed in a solvent box of TIP3P water of 20 Å (we define such systems as "free"). Such a large solvation shell (about 6000 water molecules were explicitly considered) was necessary to obtain converged results since the solute, because of its low molecular mass, tended to diffuse out or worse be at the borders of the periodic cell domain, which could result, after re-imagining the system, in partial desolvation of the investigated molecule. The same problem did not occur for the larger system comprising agarose because of its smaller mobility, determined by the larger mass. The computed interaction energies are summarized in Table 3.

Analysis of the difference of van der Waals and electrostatic energies between the free and bound ligands clearly indicates that the driving force for adsorption of A2P on agarose is van der Waals interactions, which are always larger than electrostatic interaction energies, except for A2P + SS5. In particular, the large energy difference for the A2P + SS5 system can be attributed to a very strong interaction with agarose, which leads to a partial reorganization of the support around the ligand. This structural change is of course associated with a decrease of the cohesive energy of agarose, which, if included in the calculation, would increase the interaction energy changes and, in particular, the electrostatic term.

The positive VdW interaction energy of A2P + DES, and in particular the large electrostatic term of the spacer, is determined by the particular conformation assumed by this system. As mentioned previously, in this system the spacer is interposed between ligand and support and thus interacts significantly with the support. From this derives the positive electrostatic term, which is determined by the fact that DES is a hydrophilic molecule and thus loses a significant amount of electrostatic energy passing from the solvated conformation to that in which it is adsorbed on agarose. It is also interesting to observe that for the DES + A2P system the sum of spacer and ligand interaction energies is positive, which leads one to wonder which is the driving force that leads to this conformation. This can be almost entirely ascribed to the mutual interaction between spacer and ligand, which we calculated to be −7.5 and −8.1 kcal/mol for VdW and electrostatic energies, respectively.

The small energy differences of the three LP spacers, which are characterized by a conformation in which A2P is adsorbed

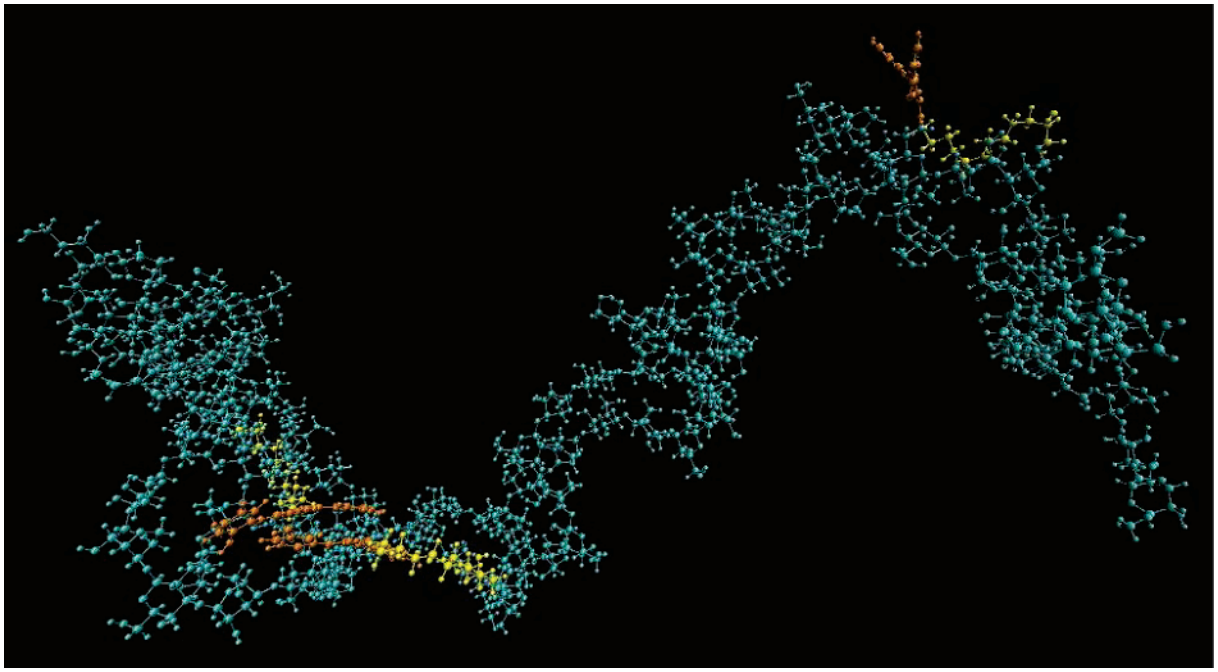

Figure 14. Final snapshot of the 5-ns simulations of three A2P ligands bound to an agarose support through a $CH_2-CHOH-CH_2-NH_2-(CH_2)_8-NH$ spacer.

TABLE 3: Calculated Interaction Energies between Bound and Free Ligand and Spacers Considered in This Study and the Environment (by environment we refer to the sum of water and agarose (if present); data reported in kcal/mol)

ligand		A2P	A2P	A2P	A2P	A2P	A2P
spacer		2LP	6LP	8LP	DES	SS3	SS5
bound spacer	electrostatic	−50.8	−47.6	−53.7	−20.8	−14.2	−16.9
	VdW	−10.4	−19.1	−18.6	−25.3	−13.7	−20.3
bound ligand	electrostatic	−51.0	−50.3	−47.1	−72.7	−71.0	−90.3
	VdW	−29.0	−35.3	−34.9	−16.2	−24.7	−29.7
free spacer	electrostatic	−49.4	−50.3	−50.8	−34.1	−15.3	−18.4
	VdW	−7.1	−14.1	−18.2	−19.2	−12.3	−17.8
free ligand[a]	electrostatic	−49.7	−49.7	−49.7	−72.9	−72.9	−72.9
	VdW	−24.3	−24.3	−24.3	−19.7	−19.7	−19.7
bound → free spacer	ΔElectro	1.4	−2.7	2.9	−13.3	−1.1	−1.5
	ΔVdW	3.3	5.0	0.4	6.1	1.4	2.5
bound → free ligand	ΔElectro	1.3	0.6	−2.6	−0.2	−1.9	17.4
	ΔVdW	4.7	11.0	10.6	−3.5	5.0	10.0

[a] The two different sets of VdW and electrostatic energy values reported for the free A2P ligands are determined by a different definition of A2P when bound to LP, which is a part of the LP spacer itself.

on agarose, indicate that their interaction with agarose is slight and of the VdW type.

As a general remark, we can observe that the data reported in Table 3 show that absolute electrostatic interaction energies between spacers and ligand and the environment are larger than van der Waals forces, which is what would normally be expected. However, the change of interaction energy between the bound and unbound state indicates that van der Waals forces play a major role. This is not surprising since IgG affinity chromatography ligands are designed to maximize the interaction with the hydrophobic binding site of the antibody, which is known as the "consensus binding site". This means that such ligands are usually hydrophobic. Thus, it is to be expected that an increase of the solvent-accessible surface of spacer and ligand will eventually lead to a decrease the van der Waals energy of interaction with the environment.

4. Summary and Conclusions

The focus of this study has been computational investigation of the nature of the interaction between an affinity ligand and the agarose support to which it was bound through spacers of different length and chemical nature. This work allowed elucidation of the effect that the use of a spacer has on development of a stable ligand−spacer−support structural conformation. In particular, the following conclusions can be drawn.

The spacer hydrophobicity significantly influences the conformational evolution of the ligand−substrate system. In particular, if the supported ligand is slightly hydrophobic, such as in A2P, its lowest energy conformation is to be adsorbed on agarose. According to MD simulations, this conformation is rapidly reached and maintained.

Use of a hydrophilic spacer can change the stable conformation of the A2P ligand from the adsorbed to the fully solvated structure. This effect is proportional to the solvation free energy of the spacer, which can thus be exploited as a parameter to modify its stable conformation.

An increase of the length of the spacer corresponds to an increase of its rotational flexibility, which can eventually lead to formation of structures where the ligand is interacting with agarose. Two structures were found. In one case the spacer arm is solvated and the ligand is adsorbed on agarose, while in the

other, which is probably metastable, the spacer is sandwiched between the ligand and the support.

Two ligands, if adsorbed on neighboring sites and if the substrate has a sufficient mobility to let them come in proximity with each other, can interact and form a complex. The energy gained by formation of such a complex can be sufficient to determine a major rearrangement of the agarose structure, if it is constituted by an unrestrained double helix.

In conclusion, the simulations have shown that agarose can interact significantly with a supported ligand. The spacer used to connect the ligand to the surface directly influences the extent of such interaction. The spacer hydrophilicity and rigidity can be used as tools to change the minimum energy conformation of the ligand with respect to the support. Computational investigations can help to design the spacer chemical structure with the best properties using its solvation free energy as a parameter and directly predicting which conformation will be reached, adsorbed or solvated, through MD simulations.

Acknowledgment. The authors are grateful to W. Lindner for continuous and fruitful discussions and, in particular, for suggesting the different spacer compositions to examine. We thank the European Commission for funding this work under the integrated project Advanced Interactive Materials by Design (contract no. NMP3-CT2004-500160).

References and Notes

(1) Van Emon, J. M.; Gerlach, C. L.; Bowman, K. *J. Chromatogr. B* **1998**, *715*, 211.
(2) Leonard, M. *J. Chromatogr. B* **1997**, *699*, 3.
(3) Tamura, T.; Terada, T.; Tanaka, A. *Bioconjugate Chem.* **2003**, *14*, 1222.
(4) Zhang, X.; Wang, J. C.; Lacki, K. M.; Liapis, A. I. *J. Phys. Chem. B* **2005**, *109*, 21028.
(5) O'Carra, P.; Barry, S.; Griffin, T. *FEBS Lett.* **1974**, *43*, 169.
(6) O'Flaherty, M.; McMahon, M.; Mulcahy, P. *Protein Expr. Purif.* **1999**, *15*, 127.
(7) Massouliè, J.; Bon, S. *Eur. J. Biochem.* **1976**, *68*, 531.
(8) McCourt, P. A. G.; Gustafson, S. *Int. J. Biochem. Cell Biol.* **1997**, *29*, 1179.
(9) Lowe, C. R. *Eur. J. Biochem.* **1977**, *73*, 265.
(10) DePhillips, P.; Lagerlund, I.; Farenmark, J.; Lenhoff, A. M. *Anal. Chem.* **2004**, *76*, 5816.
(11) Berna, P. P.; Porath, J. *J. Chromatogr. A* **1996**, *753*, 57.
(12) Liapis, A. I.; Grimes, B. A. *J. Sep. Sci.* **2005**, *28*, 1909.
(13) Newcombe, A. R.; Cresswell, C.; Davies, S.; Watson, K.; Harris, G.; O'Donovan, K.; Francis, R. *J. Chromatogr. B* **2005**, *814*, 209.
(14) Kirschner, K. N.; Woods, R. J. *Proc. Natl. Acad. Sci. U.S.A* **2001**, *98*, 10541.
(15) Case, D. A.; Darden, T. A.; Cheatham, T. E., III; Simmerling, C. L.; Wang, J.; Duke, R. E.; Luo, R.; Merz, K. M.; Wang, B.; Pearlman, D. A.; Crowley, M.; Brozell, S.; Tsui, H.; Gohlke, H.; Mongan, J.; Hornak, V.; Cui, G.; Beroza, P.; Schafmeister, C.; Caldwell, J. W.; Ross, W. S.; Kollman, P. A. *AMBER 8*, 8.0 ed.; University of California: San Francisco, 2004.
(16) Basma, M.; Sundara, S.; Calgan, D.; Vernali, T.; Woods, R. J. *J. Comput. Chem.* **2001**, *22*, 1125.
(17) Kirschner, K. N.; Woods, R. J. *J. Phys. Chem. A* **2001**, *105*, 4150.
(18) Cornell, W. D.; Cieplak, P.; Bayly, C. I.; Gould, I. R.; Merz, K. M., Jr.; Ferguson, D. M.; Spellmeyer, D. C.; Fox, T.; Caldwell, J. W.; Kollman, P. A. *J. Am. Chem. Soc.* **1995**, *117*, 5179.
(19) Bayly, C. I.; Cieplak, P.; Cornell, W. D.; Kollman, P. A. *J. Phys. Chem.* **1993**, *97*, 10269.
(20) Arnott, S.; Fulmer, A.; Scott, W. E.; Dea, I. C. M.; Moorhouse, R.; Rees, D. A. *J. Mol. Biol.* **1974**, *90*, 269.
(21) Ramzi, M.; Rochas, C.; Guenet, J. M. *Macromolecules* **1996**, *29*, 4668.
(22) Wang, J.; Wolf, R. M.; Caldwell, J. W.; Kollman, P. A.; Case, D. A. *J. Comput. Chem.* **2004**, *25*, 1157.
(23) Jorgensen, W. L.; Chandraskhar, J.; Madura, J. D.; Impey, R. W.; Klein, M. L. *J. Phys. Chem.* **1983**, *79*, 926.
(24) Case, D. A.; Cheatham, T. E.; Darden, T.; Gohlke, H.; Luo, R.; Merz, K. M.; Onufriev, A.; Simmerling, C.; Wang, B.; Woods, R. J. *J. Comput. Chem.* **2005**, *26*, 1668.
(25) Hunenberger, P. H.; McCammon, J. A. *Biophys. Chem.* **1999**, *78*, 69.
(26) Ryckaert, J. P.; Ciccotti, G.; Berendsen, H. J. C. *J. Comput. Phys.* **1977**, *23*, 320.
(27) Frisch, M. J.; Trucks, G. W.; Schlegel, H. B.; Scuseria, G. E.; Robb, M. A.; Cheeseman, J. R.; Montgomery, J. A., Jr.; Vreven, T.; Kudin, K. N.; Burant, J. C.; Millam, J. M.; Iyengar, S. S.; Tomasi, J.; Barone, V.; Mennucci, B.; Cossi, M.; Scalmani, G.; Rega, N.; Petersson, G. A.; Nakatsuji, H.; Hada, M.; Ehara, M.; Toyota, K.; Fukuda, R.; Hasegawa, J.; Ishida, M.; Nakajima, T.; Honda, Y.; Kitao, O.; Nakai, H.; Klene, M.; Li, X.; Knox, J. E.; Hratchian, H. P.; Cross, J. B.; Bakken, V.; Adamo, C.; Jaramillo, J.; Gomperts, R.; Stratmann, R. E.; Yazyev, O.; Austin, A. J.; Cammi, R.; Pomelli, C.; Ochtersk, J. W.; Ayala, P. Y.; Morokuma, K.; Voth, G. A.; Salvador, P.; Dannenberg, J. J.; Zakrzewski, V. G.; Dapprich, S.; Daniels, A. D.; Strain, M. C.; Farkas, O.; Malick, D. K.; Rabuck, A. D.; Raghavachari, K.; Foresman, J. B.; Ortiz, J. V.; Cui, Q.; Baboul, A. G.; Clifford, S.; Cioslowski, J.; Stefanov, B. B.; Liu, G.; Liashenko, A.; Piskorz, P.; Komaromi, I.; Martin, R. L.; Fox, D. J.; Keith, T.; Al-Laham, M. A.; Peng, C. Y.; Nanayakkara, A.; Challacombe, M.; Gill, P. M. W.; Johnson, B.; Chen, W.; Wong, M. W.; Gonzalez, C.; Pople, J. A. *Gaussian 03*, Revision C.01; Gaussian, Inc: Pittsburgh, PA, 2003.
(28) Schaftenaar, G.; Noordik, J. H. *J. Comput.-Aided Mol. Des.* **2000**, *14*, 123.
(29) Humphrey, W.; Dalke, A.; Schulten, K. *J. Mol. Graphics* **1996**, *14*, 33.
(30) Bosco, M.; Segre, A.; Miertus, S.; Cesaro, A.; Paoletti, S. *Carbohydr. Res.* **2005**, *340*, 943.
(31) Anderson, N. S.; Campbell, J. W.; Harding, M. M.; Rees, D. A.; Samuel, J. W. B. *J. Mol. Biol.* **1969**, *45*, 85.
(32) Xiong, J. Y.; Narayanan, J.; Liu, X. Y.; Chong, T. K.; Chen, S. B.; Chung, T. S. *J. Phys. Chem. B* **2005**, *109*, 5638.
(33) Rochas, C.; Brulet, A.; Guenet, J. M. *Macromolecules* **1994**, *27*, 3830.
(34) Kouwijzer, M.; Perez, S. *Biopolymers* **1998**, *46*, 11.
(35) Ramzi, M.; Rochas, C.; Guenet, J. M. *Macromolecules* **1998**, *31*, 6106.
(36) Cances, E.; Mennucci, B.; Tomasi, J. *J. Chem. Phys.* **1997**, *107*, 3032.